V International Conference on Particle-based Methods – Fundamentals and Applications
PARTICLES 2017
P. Wriggers, M. Bischoff, E. Oñate, D.R.J. Owen, & T. Zohdi (Eds)

INVESTIGATION OF PARTICLE PROPERTIES ON THE HOLDING FORCE IN A GRANULAR GRIPPER

Steven Meuleman[1,*], Vincent Balt[1,*], Ahmed Jarray[1,2] and Vanessa Magnanimo[1]

[1] Multi Scale Mechanics (MSM)
University of Twente, NL-7500 AE Enschede, The Netherlands.
s.meuleman@student.utwente.nl
v.a.balt@student.utwente.nl

[2] Research Center Pharmaceutical Engineering GmbH
Graz, Austria

[*] These authors contributed equally

Key words: DEM, granular gripper, surface roughness, dry friction

Abstract. The granular gripper is an innovative device designed to grasp objects using the jamming properties of granular materials. However, these properties that influence its performance is still poorly understood. Moreover, to date, there is no numerical model for the granular gripper. In this paper, we combine numerical and experimental approaches to examine the effects of the mechanical properties of the grains on the grip force, with the goal to gain better insight on the influence of these properties and to improve the performance of the granular gripper.
On the numerical side, a model based on Discrete Elements Method (DEM) is developed to predict the effect of the granular properties, such as the roughness, on the holding force. Two different ways of modelling the gripper system are presented and compared. The DEM model is tested for different pressures around the jamming pressure. On the experiment side, a granular gripper apparatus is mounted and used to find the relationship between the grains properties and the holding force. The experimental apparatus is also used to validate the DEM model.
We found that grains with higher surface roughness result in a higher holding force on a cubical aluminium object. We also found agreements between the results of the experiments and the DEM models. Lastly, advice is given about approximating the holding force for a given gripper system and about further optimizing this system in terms of holding force, pressure and particle roughness.

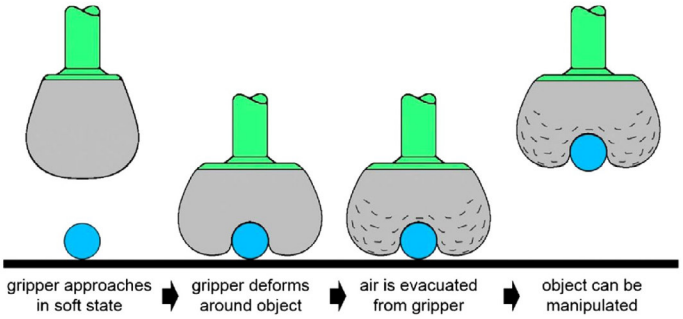

Figure 1: Functioning of the granular gripper [1].

1 Introduction

Gripping, holding and moving parts in industrial applications are tasks done by robotic grippers. Often these tasks are done by complex robotic hands which require a lot of processing power and optimization [1, 2]. However, a new and more universal way of gripping objects has come to light. A lot of complexity and therefore costs can be avoided by gripping objects using a granular gripper [1, 2, 3]. The functioning of the granular gripper consists of four phases which are shown in figure 1. The holding force that is exerted on the object has three contributions, static friction from surface contact, geometrical interlocking and vacuum suction from an airtight seal [2]. This research will mainly focus on the static friction contribution. The holding force at jamming pressure can be used to determine the performance of a granular gripper. The jamming point, the jamming transition from a fluid-like state of the granular material to a solid-like state occurs at this jamming pressure [4]. Optimization of the granular gripper will help improving its performance and therefore its usability. Discrete element method modelling is a useful tool for this optimization problem. In DEM modelling deformations of particles are simplified to the overlap, δ, of two particles which corresponds to an interaction force [5].

So far ground coffee is found to have the best properties for a high strength-to-weight ratio. A property that is used to measure the performance of systems containing granular material [3], like the gripper. A hypothesis for this is the influence of the surface roughness and irregularities [3], because ground coffee is relatively rough and non-spherical compared to other granular media such as glass beads for example. In order to explore the influence of roughness on the gripper performance, the problem is studied by combining gripper experiments, microscope image analysis on single particles roughness and numerical simulations. A roughness experiment is first conducted to identify the roughness of different batches of particles by taking samples. Also from the other batches of particles containers are filled and tested in the granular gripper set-up. Then, the roughness is examined against the holding force in the granular gripper and an implementation of the roughness in the simulation is established.

2 Roughness experiment

2.1 Method

Samples of Silibeads® Type M Borosilicate glass beads with a diameter of $2.5 \pm 0.2\ mm$ are tested. Both a matte as well as a polished type is used in the experiments. The experiment is conducted using the Keyence VK-9700 series Color 3D Laser Scanning Confocal Microscope. The microscope is used with the laser shutter as well as the aperture shutter opened. The lens with 100x magnification was used for making surface measurements of the centre of the particle surface. Afterwards the results are processed by the VK Analyser software that comes with the microscope. In this software, the scanned surface is flattened using the "sec curved surf.(auto)" correction method. The value for RMS_f is then found by taking the root mean squared roughness of the whole measured surface which is about 105 μm x 140 μm. After each experiment, it is made sure that the same bead is not used again in any later experiment. By linear fitting measurement data from [6] the following approximation is found for the mean RMS_f value in micrometers and the static coefficient of friction μ_s:

$$\mu_s = 2.012 \cdot RMS_f - 0.0026 \tag{1}$$

2.2 Results

Type	Mean RMS_f $[\mu m]$	St. dev. $[\mu m]$
polished 2.5 mm	0.060	0.016
polished 4 mm	0.152	0.028
matte 2.5 mm	0.458	0.018
matte 4 mm	1.063	0.122

Table 1: Surface roughness results for the flattened plane RMS roughness, RMS_f for a surface of 105 μm x 140 μm.

Type	Mean coefficient
polished 2.5 mm	0.12
polished 4 mm	0.3
matte 2.5 mm	0.92
matte 4 mm	2.14

Table 2: Mean static friction coefficient, μ_s, approximation using equation (1).

In table 1 the average flattened RMS surface roughness values can be found. For each type 6 experiments are conducted. The standard deviation from the mean is also shown as a measure of accuracy. In figure 2 examples of typical tested surfaces for the respective

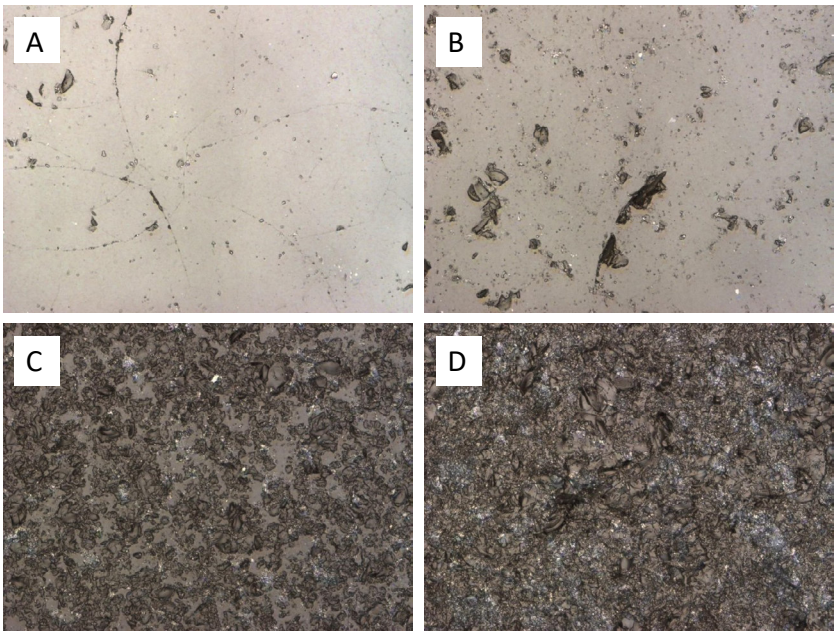

Figure 2: Microscopical view of the surface of the samples. A: polished 2.5 mm, B: polished 4 mm, C: matte 2.5 mm, D: matte 4 mm.

types are shown which consists of two layers. The first layer is the coloured view from the microscope and the second view is the laser view. The flattened RMS surface roughness values are filled into equation (1) to approximate the static friction, μ_s. The result can be found in table 2. Since the friction values in [6] did deviate much at the same roughness, this friction value is only an indication.

2.3 Conclusions & discussion

In table 1 it can be seen that the matte Silibeads® Type M Borosilicate glass beads have a higher RMS_f value than the polished ones. This difference is also expected for the static friction, μ_s, values. A bigger diameter results in a higher RMS_f value and therefore also a higher static friction, μ is expected.

3 Model validation

3.1 Method

A model of the granular gripper set-up is made to simulate the holding force. Firstly, some experiments are conducted using the experimental set-up. Then in the simulation the same experiment is conducted. Afterwards the results are compared. The DEM software that is used for doing the simulations is LIGGGHTS®-PUBLIC version 3.5 [7]. The contact model that is used for all contacts is the Hertz model combined with the tangential history model. For the contact between the aluminium cube and the particles,

a function "limitForce" was used to prevent attractive forces which is unwanted behaviour [8]. Both models and the function are included in the software. In both the experiment and the simulation, the holding force is determined by taking the highest force value that occurred while being in the upward motion. The residuary settings of both the set-up and the model will now be discussed.

The polished & matte Type M borosilicate 2.5 mm particle types from section 2 are used for model verification. For every particle type one or two containers are utilized in the experimental set-up. The weight for every container filled with particles is tested not to differ more than 10 $grams$ from the measured average of 310 $grams$. It is chosen to do this for a more accurate performance comparison between the types. In the simulation, the friction coefficient values from table 2 are used for the holding force comparison.

3.1.1 Experimental set-up

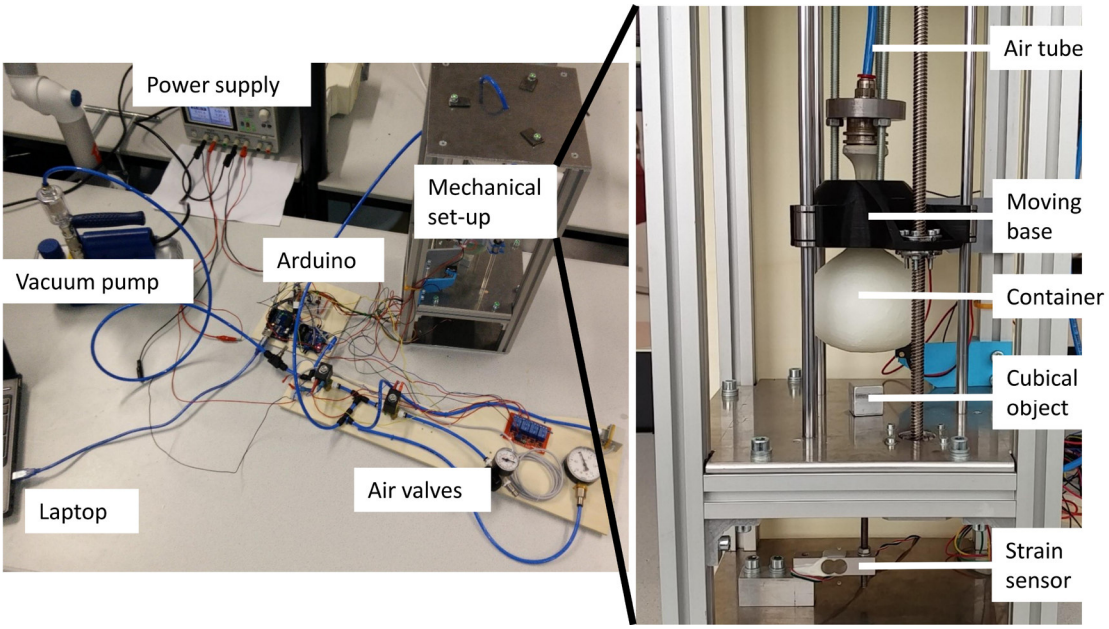

Figure 3: On the left: total set-up, on the right: mechanical part of the set-up.

Property	Value	Unit
Particle diameter	0.0025	m
Bellow radius	0.025	m
Total mass particles	0.310 ± 0.010	kg

Table 3: Properties used in the experiment.

The experimental set-up consists of a latex container with an empty weight of 3 *grams* containing the granular material. The latex container is connected to a vacuum pump which can generate a compressive pressure on the container, see figure 3. When doing experiments the vacuum pump was put on another table to reduce vibrations. Additionally, the mechanical part of the set-up was placed on a piece of foam to damp vibrations.

The latex container is connected to a frame which can be seen on the right side of figure 3 by means of a stepper motor and bearings, so the upward and downward movement can be controlled. Below the latex container, an aluminium cube is located which is connected to a force sensor. The stepper motor and air valves are controlled by an Arduino board and the sensor output is sent to a computer where the data can be analysed. The properties of the particles used are shown in table 3.

The Arduino script consists of six separate phases. In the first phase, the container moves to the reference position at the top of the set-up. In the second phase, the offset for the sensor values are calculated and implemented in the script. In the third phase, a negative pressure of $40kPa$ is applied, which is then released back to $0kPa$. This is repeated once to obtain a better packing and make the packing independent of previous cycles. In the fourth phase, the container moves down onto the object which is connected to a micro load cell. Then in the fifth phase, a negative pressure is applied to get the particles into the jammed state. When the target pressure is reached, the particles get some time to settle and then a negative pressure is applied twice again. This is to ensure the container has the right pressure and the particles had enough time to settle. Then in phase six, the container moves up and the holding force is measured. This movement is slower compared to the upward movement to allow for more precise measurements. This cycle is repeated 9 times. The maximum operating pressure that can be reached using this set-up is $85kPa$.

3.1.2 Simulation properties

First, the results of the granular gripper simulation are matched to the results of the experiment. Afterwards the influence of a variety of properties on the holding force is tested in the simulation. The simulation consists of the same phases as the Arduino script used in the experiment, described in section 3.1.1, except for reapplying the pressure and resetting the pressure.

The material specific properties that are used in this simulation are shown in table 4. Since the width/length ratio of the particles is between 0.96 and 1 according to [9] and because in the simulation there is no effective way of modelling different width/length ratios, a perfectly round sphere with a width/length ratio of 1 is modelled. The static friction value, μ_s, for the latex container - particle contact is about 2 (although it depends on the applied normal force) according to the sliding test in [10]. However, friction values can be different for different surfaces of the same material and it can also behave differently in simulation, therefore it is decided to use a value for the friction that is at maximum 5

Property	Value	Unit	Src
E-modulus	$6.40 \cdot 10^{10}$	N/m^2	[9]
Specific weight	2230	kg/m^3	[9]
Width/length ratio	1	–	[9]*
Container - particle μ_s	0.40	–	[10]*
Glass Poisson's ratio	0.2	–	[11]
Glass - glass COR	0.95	–	[12]
Glass - glass μ_s	0.94	–	[13]*

Table 4: Material specific properties used in simulation.

Property	Value	Unit
Cube edge length	0.02	m
Particle diameter	0.0025	m
Container edge length	0.04	m
Neighbor distance	0.0015	m
Time-step	$1.2 \cdot 10^{-7}$	s
Insertion and settle time	0.0240	s
Move up time	0.0312	s
Settling time	0.0432	s
Move down time	0.382	s

Table 5: Time and distance properties used in simulation.

times smaller or bigger than the values found in literature. To match the results of the experiments it is chosen to lower the container - particle friction value to 0.4, since the holding forces experienced in the experiments are much smaller than the holding forces in the simulation. Information about measurements of the static friction, μ_s, between aluminium and latex surfaces, which is the contact between the cube and the container could not be found. For the container - cube contact no accurate μ_s value could be found. Therefore, the particle - container - cube contact μ_s value will be determined by the container - particle friction used to match the simulation to the experiment.

The time and distance properties used in the simulation are shown in table 5. The phases of the simulation are inserting the particles, settling, moving up the cube, applying the pressure, settling and finally moving the cube down. These six phases are similar to the phases of the experiment, except the simulations are not consecutive and therefore no positive pressure is applied and the negative pressure is only applied once. The time-step is checked to be smaller than 15% of the Rayleigh- and Hertz time to ensure an accurate simulation. The four factors that influence the simulation time most are found to be the total number of particles, the amount of neighbours per particle (particles within neighbour distance), the total time and the time-step. Therefore, the minimum possible values of these properties for accurate simulation will be used to save computation time.

3.1.3 Modelling the latex container for different pressures

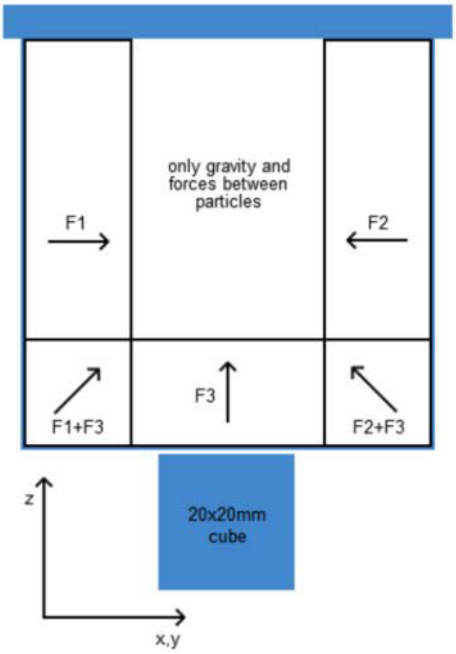

Figure 4: The "wallforces" approach.

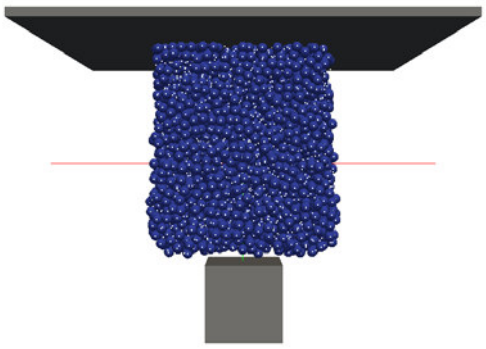

Figure 5: The model of the granular gripper

When the pressure is applied to the container, the container shrinks, exerts force on the particles that are in touch with it and deforms around them. LIGGGHTS® makes use of fixed walls and does not have the option to make a container that deforms under load. So, to model the container at different air pressure differences between the inside and the outside of the container, another approach is needed. The sides of the container are modelled with forces on particles in certain regions. These "wallforce"-regions are located at the sides of a cubical container. The "wallforces" that act on the particles in these regions have a direction towards the centre of the cube see figure 4. Because they have overlap in the lower corners of the cube the wallforces will be summed. All shown "wallforces" in figure 4 have the same magnitude. The magnitude of the "wallforces" is determined by multiplying the desired pressure with the surface area of the container and dividing it by the number of particles that experience a "wallforce". The "wallforces" approach is more like the deformation of the latex container compared to a fixed wall approach. Because with the "wallforces", the total shape of the latex container can change but it will result in stresses which is also the case for a latex container experiment. A cubical container is chosen in the simulation because only one direction for the force per "wallforce" can be chosen. The upper wall is the only wall where no "wallforce" is acting. Instead a plate that moves downward progressively based on the force that is applied on it is put there to keep the pressure inside the container constant, see figure 5.

When the container is moving to the upper reference position in the experiment (phase six of the Arduino script and of the simulation), the particles do not completely fill up the space where the cube used to be since the particles are in jammed state. To model this effect of the container between the aluminium cube and the particles when the cube is moving down, the "wallforces" approach is also applied here but with the forces directing outwards.

3.2 Results

3.2.1 Experiment

In figure 6 and figure 7 the holding force is shown for 2.5mm smooth and 2.5mm matte particles respectively at different operating pressures. At each pressure 9 experiments, shown in dark grey, are conducted consecutively. Furthermore, at each pressure 5 simulations with different insertion patterns are conducted. The small lines show the standard deviation. For both experiments and simulations, the median value is used for plotting the bars. A typical result for an experiment run is shown in figure 9. This graph shows a steady increase in the holding force as the container moves upwards. Then when the limit of the holding force is reached, the container suddenly dispatches from the cube.

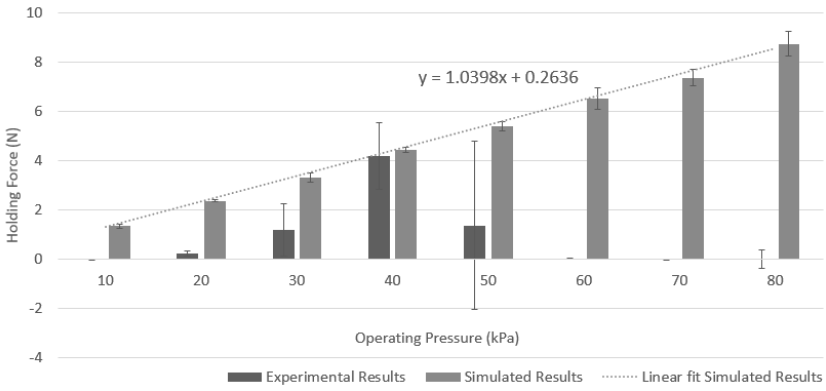

Figure 6: The holding force as a function of the operating pressure. The container is filled with 2.5mm smooth particles in both the experiments and the simulations.

.

The force values shown in figures figure 6 and figure 7 seem to be rising steadily from 0 to 40kPa and then suddenly disappears.

3.2.2 Simulation

In figure 8 a typical result for a simulation is shown. Compared to figure 9, there is a difference in the time scale because of the computation time reduction. The line is plotted at the moment the cube starts moving down (phase 4 of the Arduino script). In

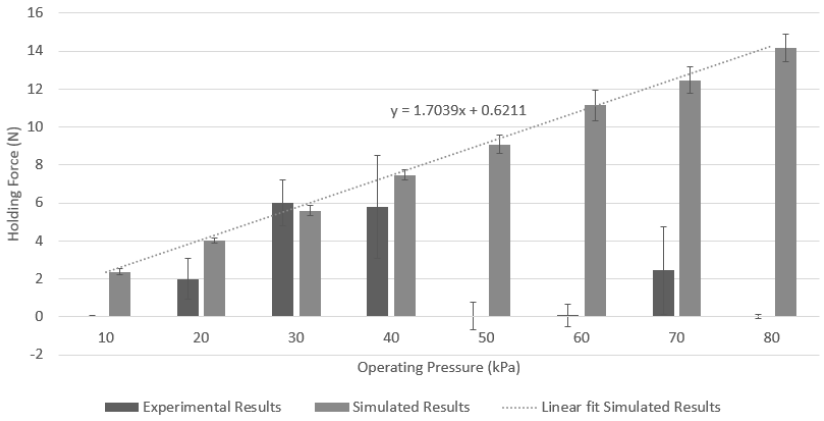

Figure 7: The holding force as a function of the operating pressure. The container is filled with 2.5mm matte particles in both the experiments and the simulations.

.

the simulation, the container does not suddenly dispatch from the cube due to the way the movement is modelled. In the simulation, the cube moves down following a cosine like path whereas in the experiment, the container only starts moving when the maximum holding force is reached and it then suddenly dispatches. In figure 6 and figure 7 the peak holding forces of the simulation for different pressures are shown. A linear fit is made of the data of which the equation can also be found in figures 6 and 7.

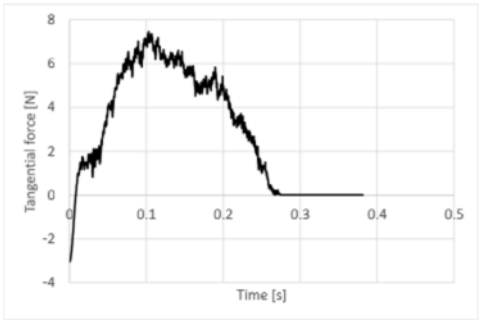

Figure 8: Holding force simulation at 40 kPa

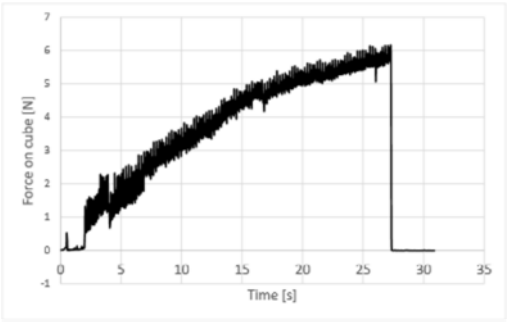

Figure 9: Holding force experiment at 40 kPa

3.3 Conclusions

Although 9 experiments are conducted for each pressure in the experimental set-up and the median is taken to exclude outliers, shown in figure 6 and figure 7, a jamming pressure could not be found since the data does not seem to follow a trend. The simulation data, however, follows a linear trend. When looking at the holding forces around 40kPa, the forces of the simulation appear to be in the same order of magnitude as the experiments.

Although the holding force of the simulation does not correspond over the entire range of operating pressures to the holding force in the experiments, the increase in holding force from matte compared to polished particles as seen in the experiments is also visible in the simulation results.

Furthermore, the matte particles result in a higher holding force compared to the smooth particles in both the simulations, as well as in the experiments.

3.4 Discussion

A possible explanation for the reduction in holding force at higher pressures shown in figures 6 and 7, is that due to the larger pressure, the container is stretched more and therefore the friction of the container is reduced. However, this does not explain why the holding force drops to 0 at higher pressures. Since there is no clear trend that can be determined from the experiments, these results are assumed to be not reliable by the authors.

Figures 6 and 7 show that the holding force as function of the operating pressure in the simulations follows a clear linear trend, which seems plausible.

4 Outlook

Even though a large amount of time is spent on examining the cause of the large deviations and the absence of a clear trend in the holding force, no cause is found. Advised is to look at alternatives for the container, for example thicker ones.

REFERENCES

[1] E. Brown, N. Rodenberg, J. Amend, A. Mozeika, E. Steltz, M. R. Zakin, H. Lipson, and H. M. Jaeger, Universal robotic gripper based on the jamming of granular material, *Proceedings of the National Academy of Sciences*, (2010), 107(44):18809–18814.

[2] John R. Amend, Eric Brown, Nicholas Rodenberg, Heinrich M. Jaeger, and Hod Lipson, A positive pressure universal gripper based on the jamming of granular material, *IEEE Transactions on Robotics*, apr 2012, 28(2):341–350.

[3] Nadia G. Cheng, Maxim B. Lobovsky, Steven J. Keating, Adam M. Setapen, Katy I. Gero, Anette E. Hosoi, and Karl D. Iagnemma, Design and analysis of a robust, low-cost, highly articulated manipulator enabled by jamming of granular media, *Proceedings - IEEE International Conference on Robotics and Automation*, (2012), 4328–4333.

[4] Stefan Luding, Granular matter: So much for the jamming point, *Nature Physics*, (2016), 1–2.

[5] Stefan Luding, Introduction to discrete element methods: basic of contact force models and how to perform the micro-macro transition to continuum theory, *European Journal of Environmental and Civil Engineering*, (2008), 12(7-8):785–826.

[6] C. O'Sullivan, M. Coop, and I. Cavarretta, The influence of particle characteristics on the behaviour of coarse grained soils, *Géotechnique*, (2010), 60(6):413–423.

[7] Christoph Kloss, Christoph Goniva, Alice Hager, Stefan Amberger, and Stefan Pirker, Models, algorithms and validation for opensource dem and cfd–dem, *Progress in Computational Fluid Dynamics, an International Journal*, (2012), 12(2-3):140–152.

[8] JKU Linz DCS Computing GmbH and Sandia Corporation, Gran model hertz model, (2016).

[9] Sigmund Lindner GmbH, SiLibeads Glass beads Type M Borosilicate, Microglass beads Product Data Sheet, (2016).

[10] Ari J. Tuononen, Onset of frictional sliding of rubber-glass contact under dry and lubricated conditions, *Scientific Reports*, (2016), 6(April):27951.

[11] G N Greaves, A L Greer, R S Lakes, and T Rouxel, Poisson's ratio and modern materials, *Nature Materials*, (2011), 10(11):823–837.

[12] Martin C Marinack Jr., Richard E Musgrave, and C Fred Higgs, Experimental investigations on the coefficient of restitution of single particles, *Tribology Transactions*, (2013), 56(4):572–580.

[13] Raymond A. Serway, *Physics for Scientists and Engineers*, Harcourt College Pub, 4 edition, (1999).